Global distribution of hydrologic controls on forest growth

Casper T. J. Roebroek[1], Lieke A. Melsen[1], Anne J. Hoek van Dijke[1,2,3], Ying Fan[4], and Adriaan J. Teuling[1]

[1]Hydrology and Quantitative Water Management Group, Wageningen University & Research, Wageningen, the Netherlands
[2]Laboratory of Geo-Information Science and Remote Sensing, Wageningen University & Research, Wageningen, the Netherlands
[3]Environmental Sensing and Modelling, Environmental Research and Innovation Department, Luxembourg Institute of Science and Technology (LIST), Belvaux, Luxembourg
[4]Department of Earth and Planetary Sciences, Rutgers University, New Brunswick, NJ 08854, USA

Correspondence: Adriaan J. Teuling (ryan.teuling@wur.nl)

Text S1: Landscape classification

The global map with landscape classes is based on the water table depth data of Fan et al. (2017). On this datasets two filters were applied; a mean (μ) and a standard deviation (σ) kernel with a window size of 5 grid cells. These two maps were combined with the decision tree as shown in Figure S7. Wetlands (and open water) are classified according to the threshold chosen by Fan et al. (2013). The other classes are separated based on the local standard deviation with the following rational. (1) Water table depth mirrors altitude, especially in hilly and mountainous areas. (2) The standard deviation is a measure of the slope of the terrain. (3) Even in the Himalayas, every window of 5 by 5 grid cells contains a cell with surface water; with the rule that the maximum range should be 6 times the standard deviation, the highest class (High mountainous) should cover both surface water and a mountain of at least a 900 meters high. It is a relatively rough classification but it is visually acceptable when compared to global maps of wetlands and digital elevation models. Changing the thresholds in the decision tree did not substantially change the main conclusions of the paper. The final map with landscape classes is shown in Figure S6.

References

Beck, H., Zimmermann, N., McVicar, T. R., Vergopolan, N., Berg, A., and Wood, E. F.: Present and future Köppen-Geiger climate classification maps at 1-km resolution, Scientific Data, 5, 1–12, https://doi.org/10.1038/sdata.2018.214, http://dx.doi.org/10.1038/sdata.2018.214, 2018.

Fan, Y., Li, H., and Miguez-Macho, G.: Global Patterns of Groundwater Table Depth, Science, 339, 940–943, https://doi.org/10.1126/science.1229881, http://www.sciencemag.org/cgi/doi/10.1126/science.1229881, 2013.

Fan, Y., Miguez-Macho, G., Jobbágy, E. G., Jackson, R. B., and Otero-Casal, C.: Hydrologic regulation of plant rooting depth, Proceedings of the National Academy of Sciences, 114, 10 572—-10 577, https://doi.org/10.1073/pnas.1712381114, https://www.pnas.org/content/114/40/10572, 2017.

Fick, S. E. and Hijmans, R. J.: WorldClim 2: new 1-km spatial resolution climate surfaces for global land areas, International Journal of Climatology, 37, 4302–4315, https://doi.org/10.1002/joc.5086, http://doi.wiley.com/10.1002/joc.5086, 2017.

Myneni, R., Knyazikhin, Y., and Park, T.: MCD15A3H MODIS/Terra+Aqua Leaf Area Index/FPAR 4-day L4 Global 500m SIN Grid V006 [Data set], https://doi.org/10.5067/MODIS/MCD15A2H.006, 2015.

Simard, M., Pinto, N., Fisher, J. B., and Baccini, A.: Mapping forest canopy height globally with spaceborne lidar, Journal of Geophysical Research, 116, 4021, https://doi.org/10.1029/2011JG001708, https://agupubs.onlinelibrary.wiley.com/doi/full/10.1029/2011JG001708, 2011.

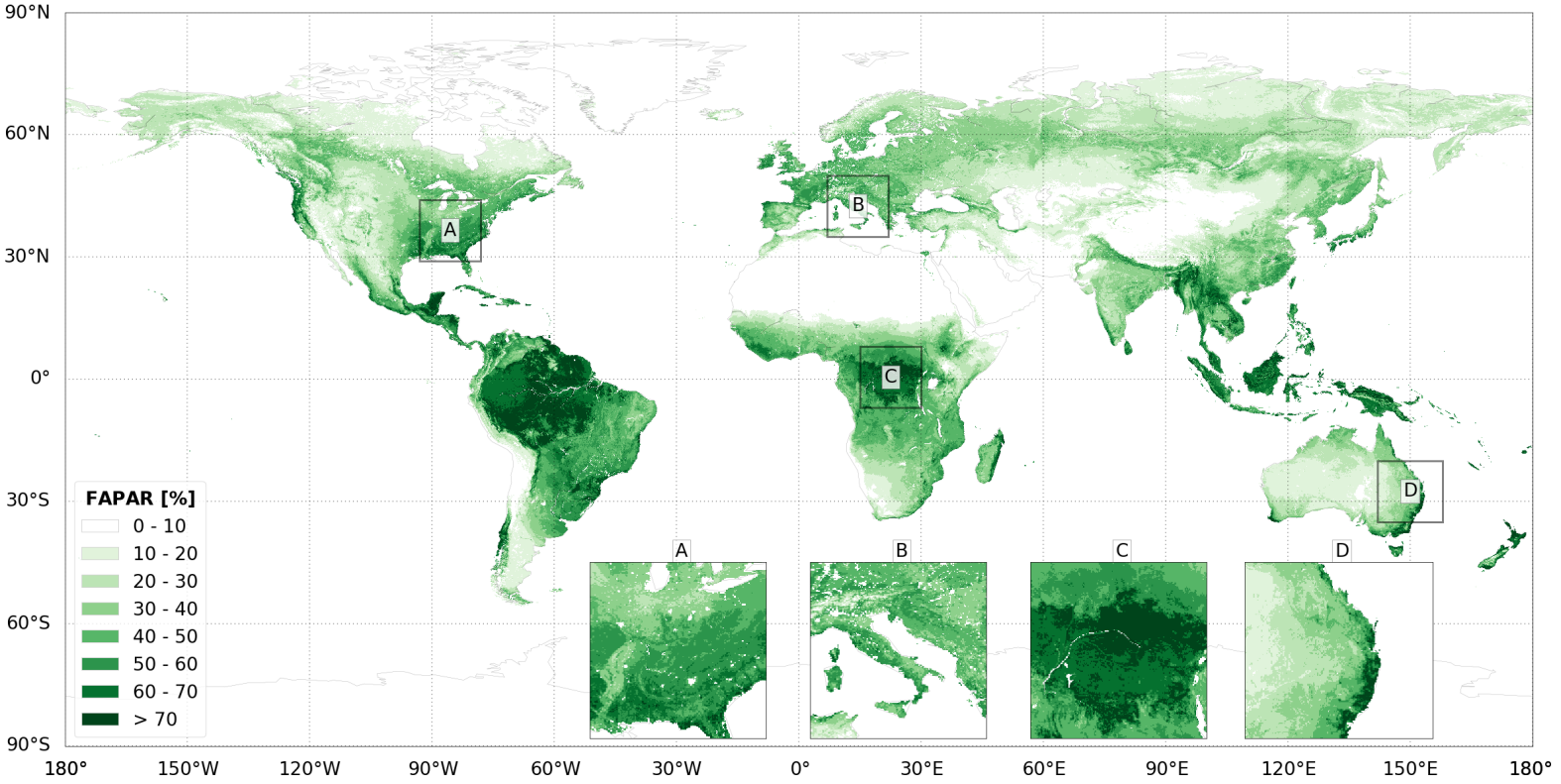

Figure S1. Global distribution of the fraction of absorbed photosynthetically active radiation (fAPAR) Myneni et al. (2015)

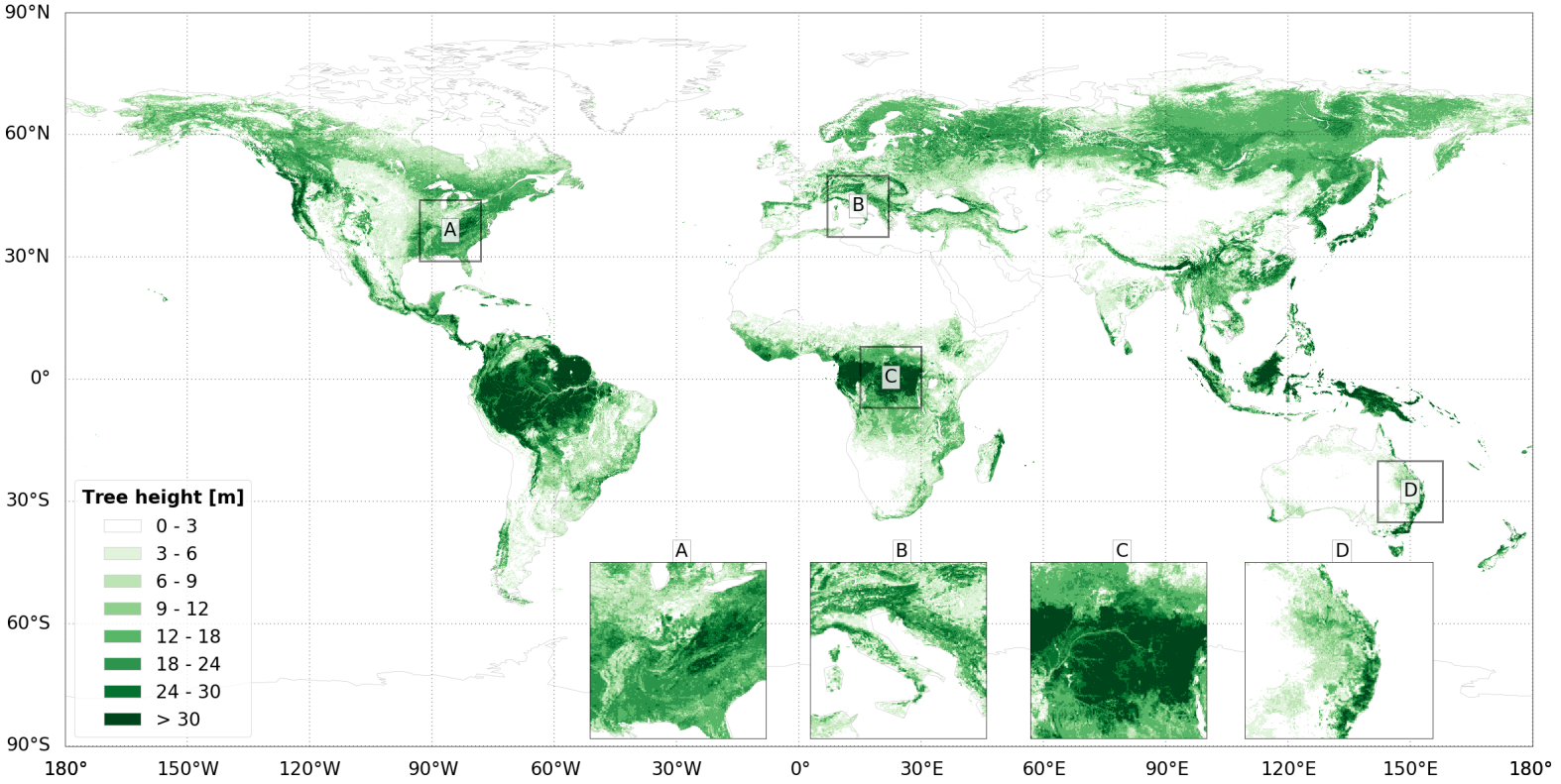

Figure S2. Global distribution of tree height Simard et al. (2011)

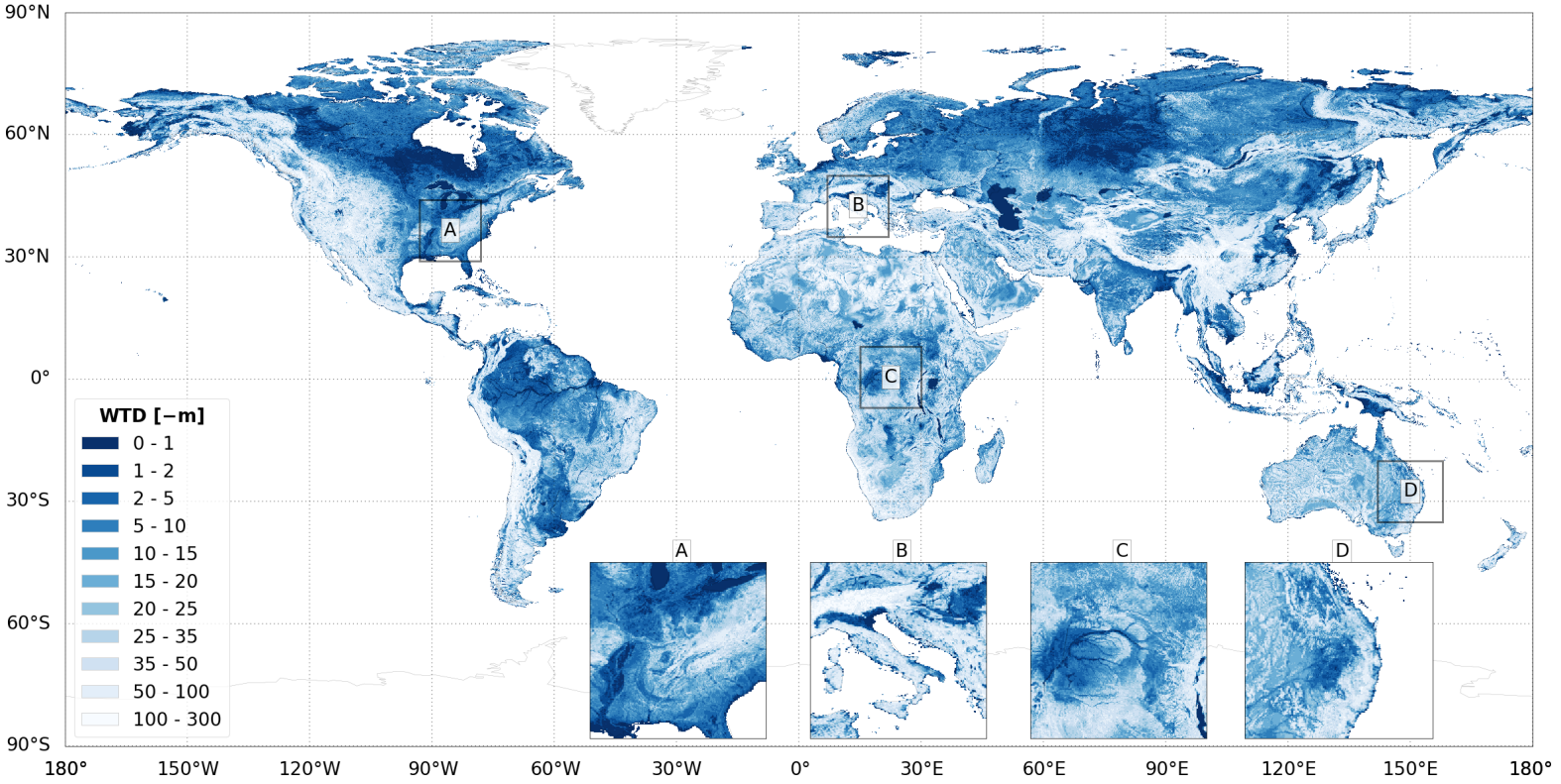

Figure S3. Global distribution of water table depth Fan et al. (2017)

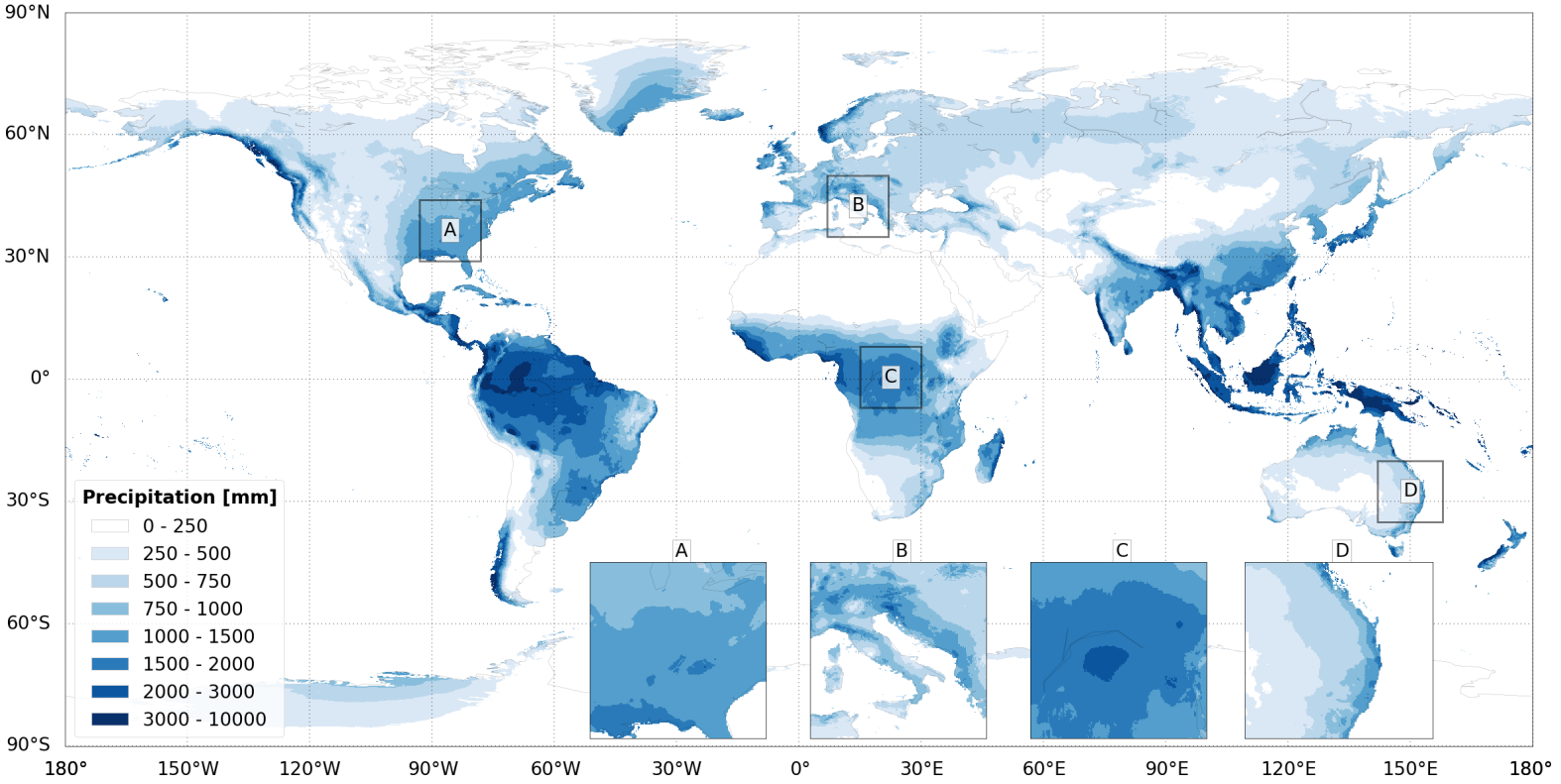

Figure S4. Global distribution of precipitation Fick and Hijmans (2017)

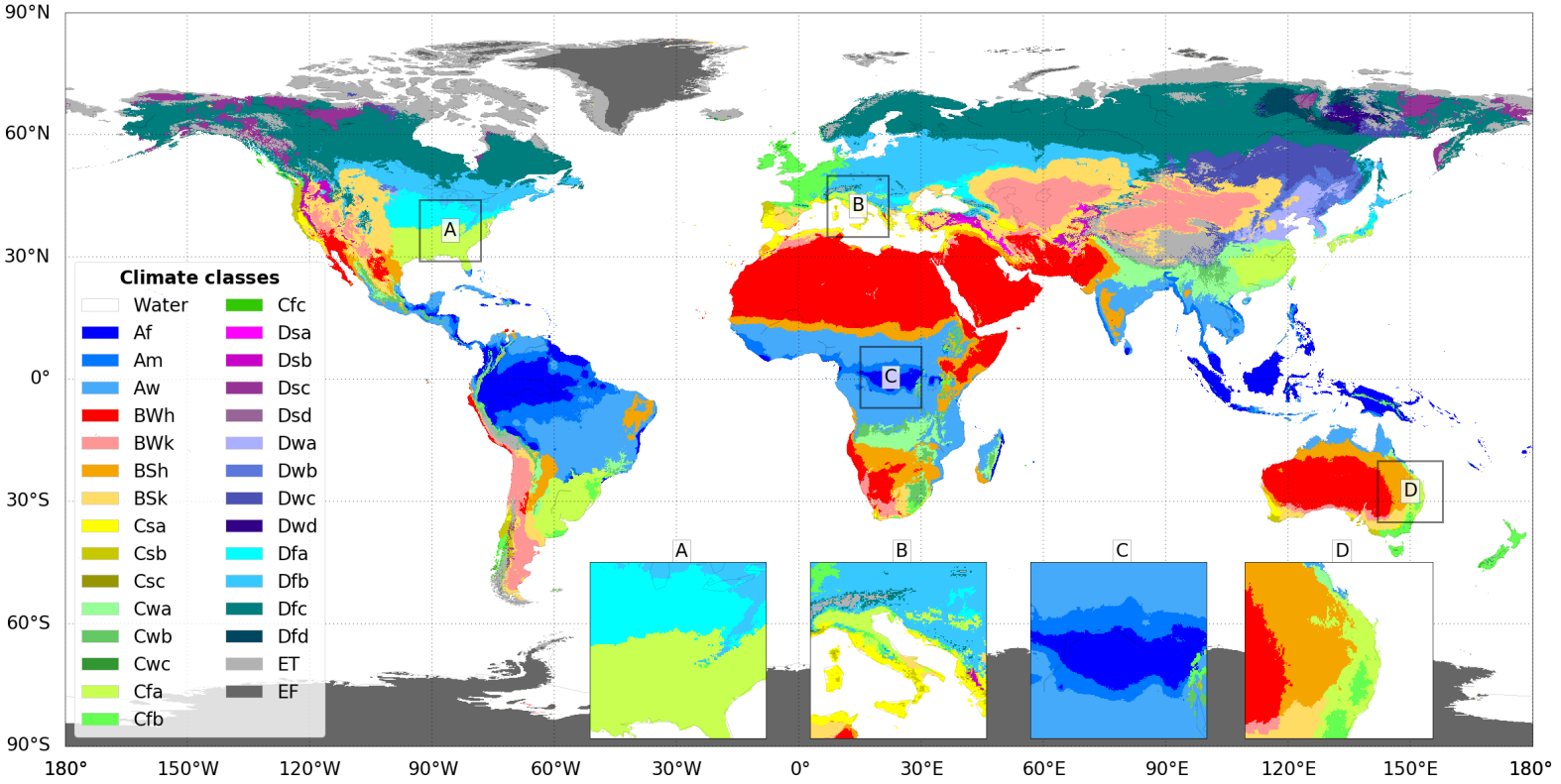

Figure S5. Global distribution of Köppen-Geiger climate classes Beck et al. (2018)

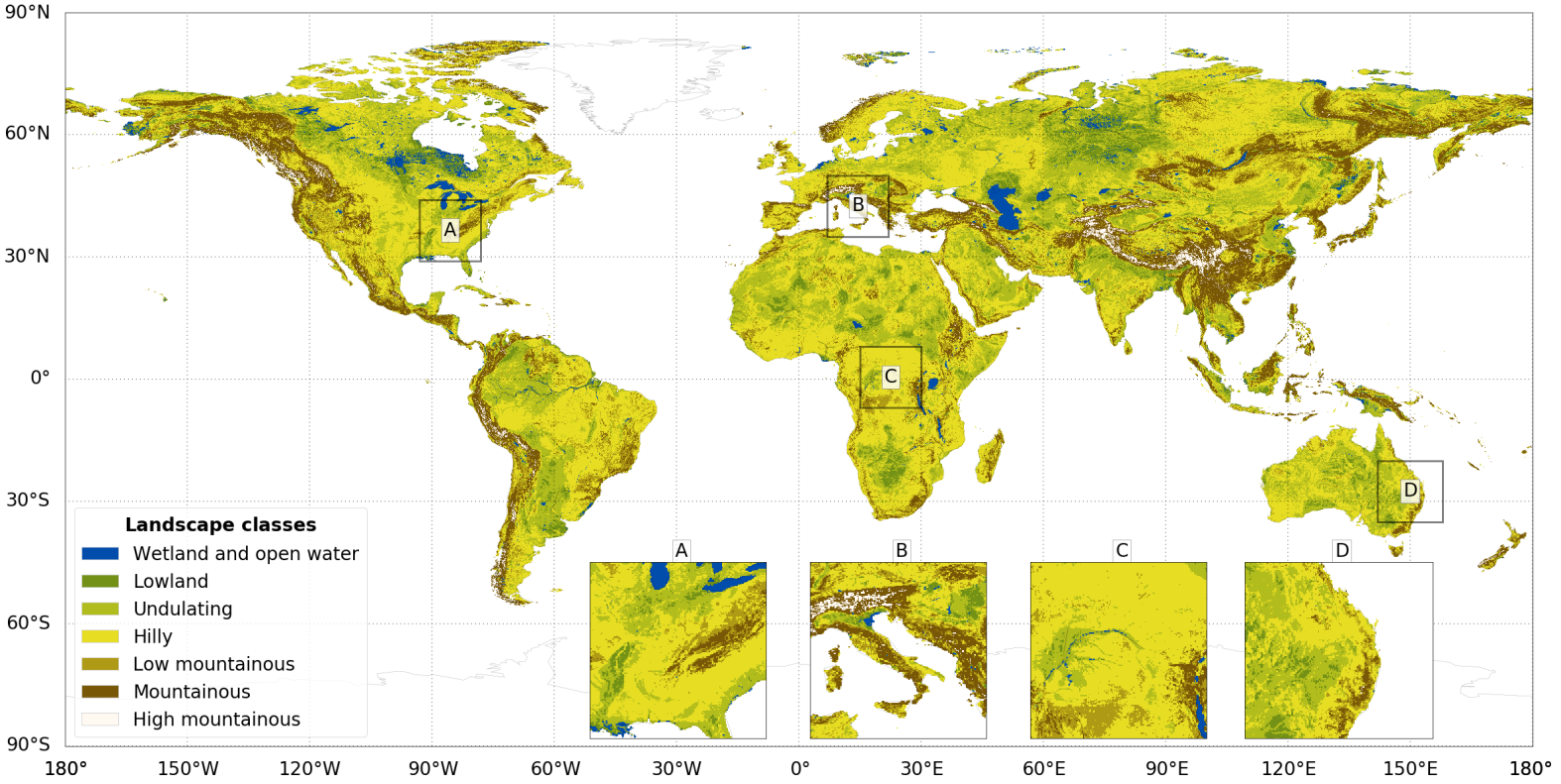

Figure S6. Global distribution of landscape classes (see Text S1 and Figure S7) for detailed explanation.

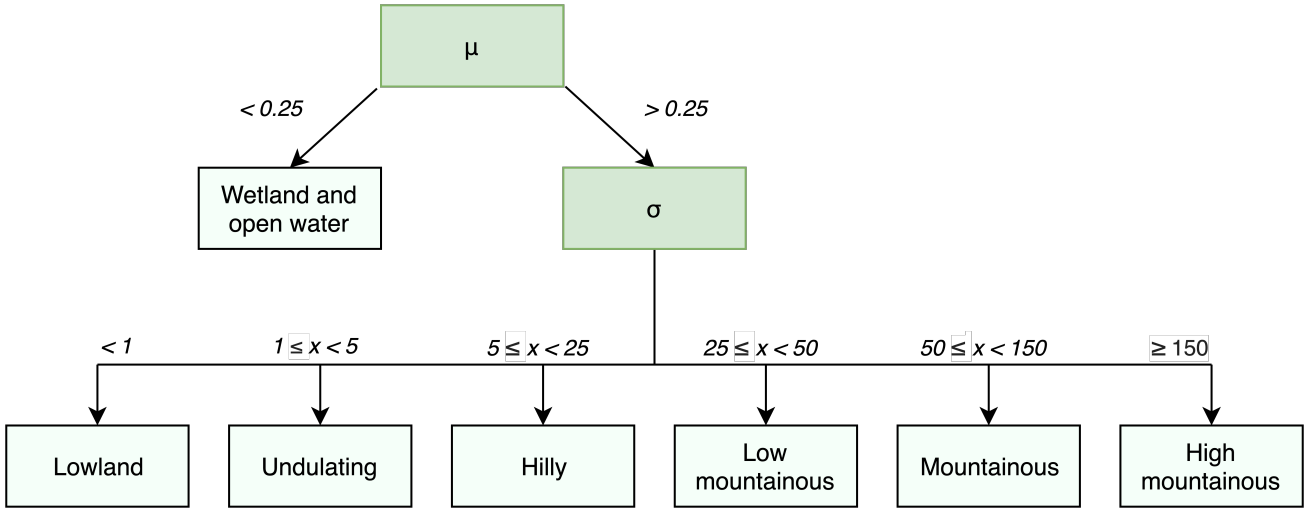

Figure S7. Decision tree used to create global landscape classes as depicted in Figure S6. The building blocks μ and σ are two datasets created by applying a sliding windows on the dataset of water table depth depicted in Figure S3. μ corresponds with a mean kernel, σ with a standard deviation kernel.

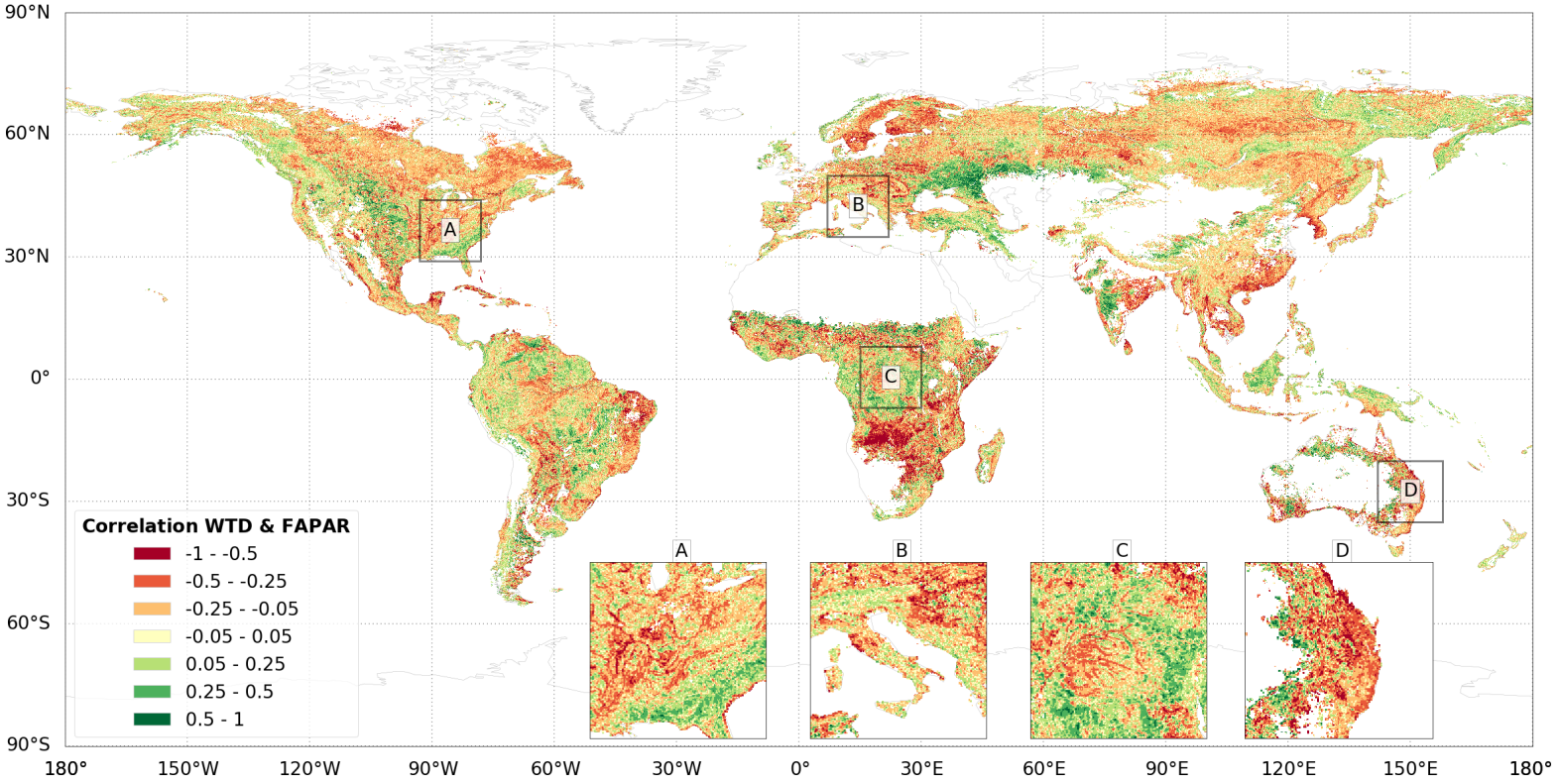

Figure S8. Global distribution of the correlation between water table depth and fAPAR.

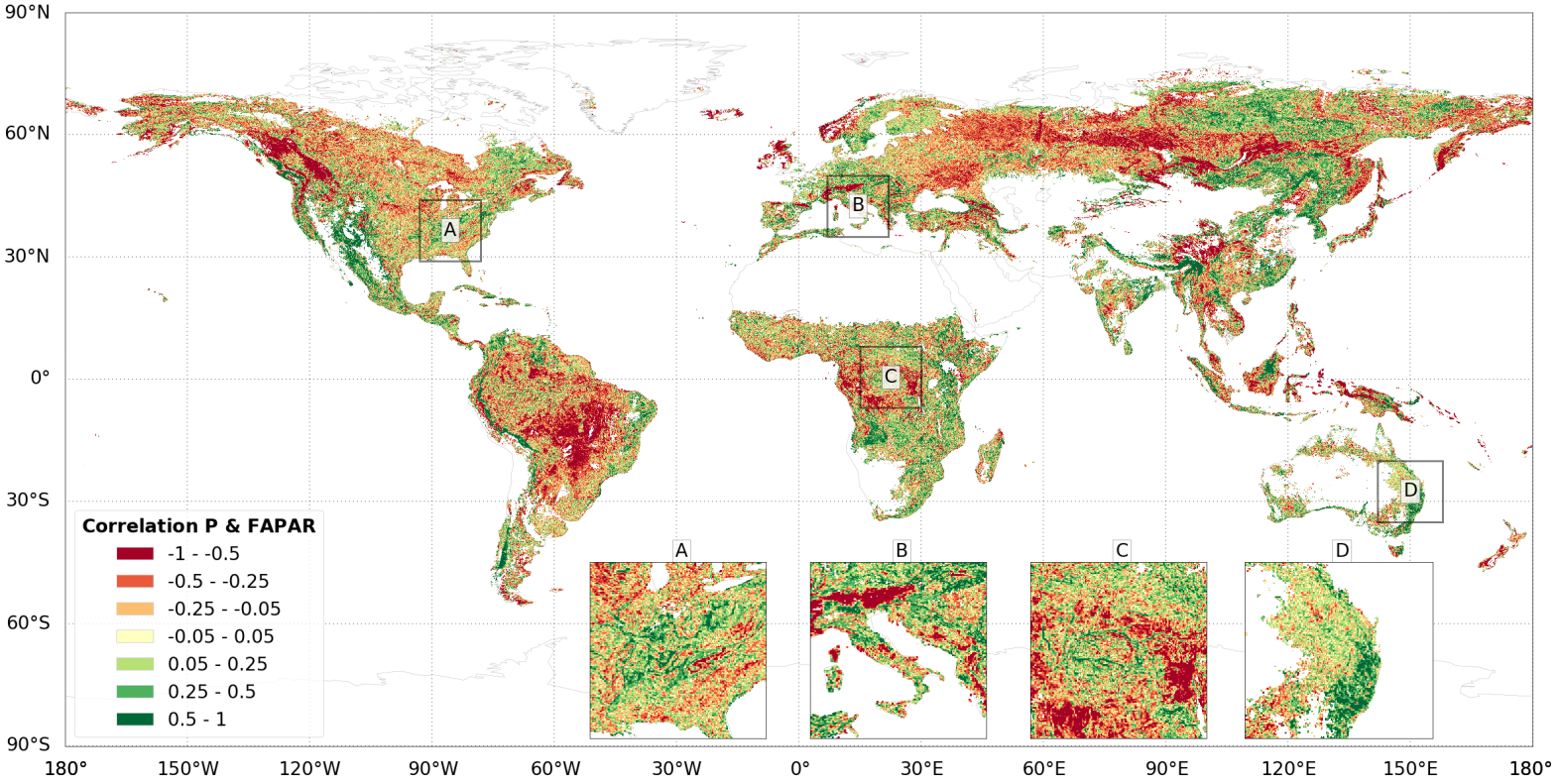

Figure S9. Global distribution of the correlation between precipitation and fAPAR.

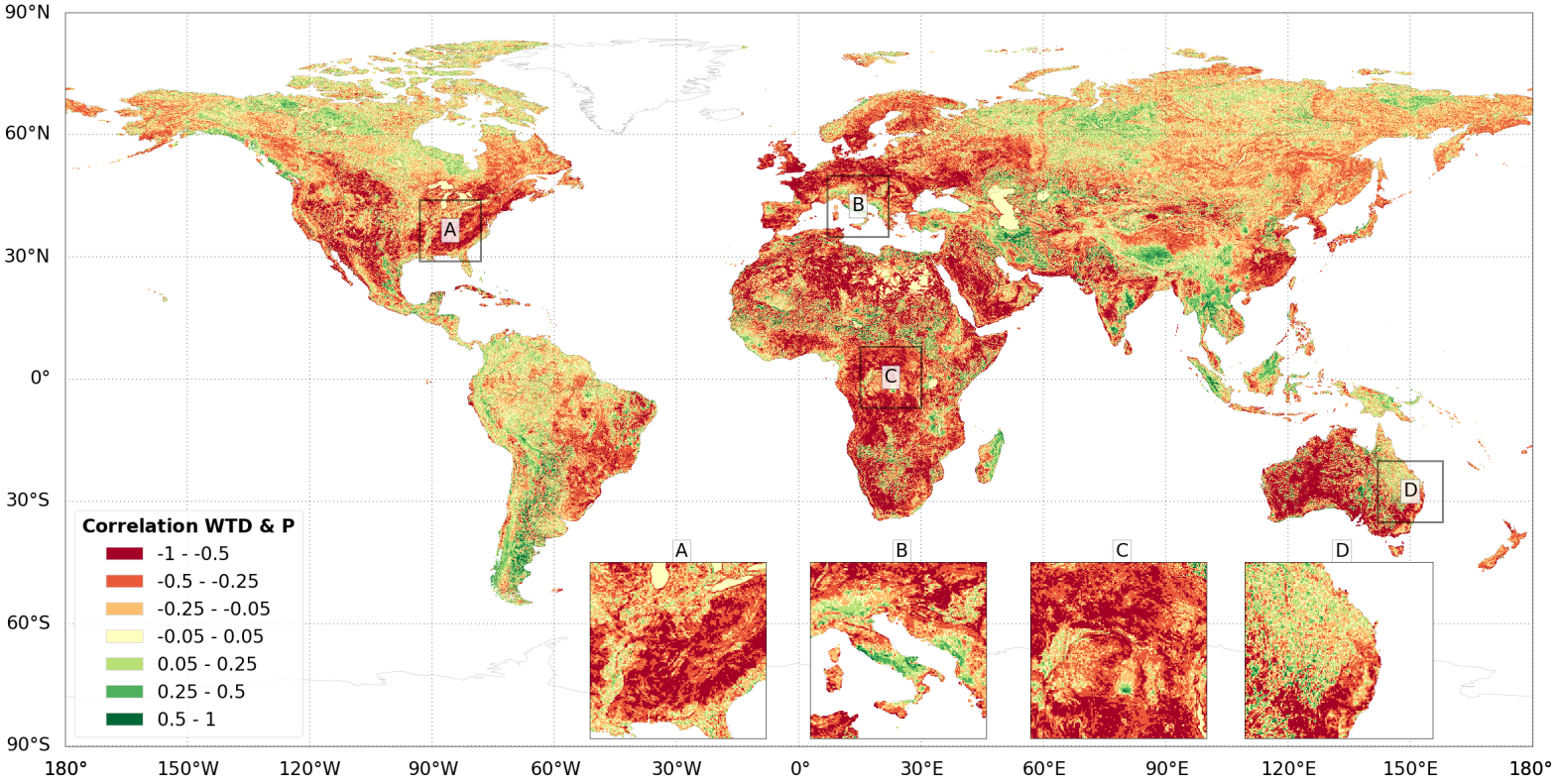

Figure S10. Global distribution of the correlation between water table depth and precipitation.

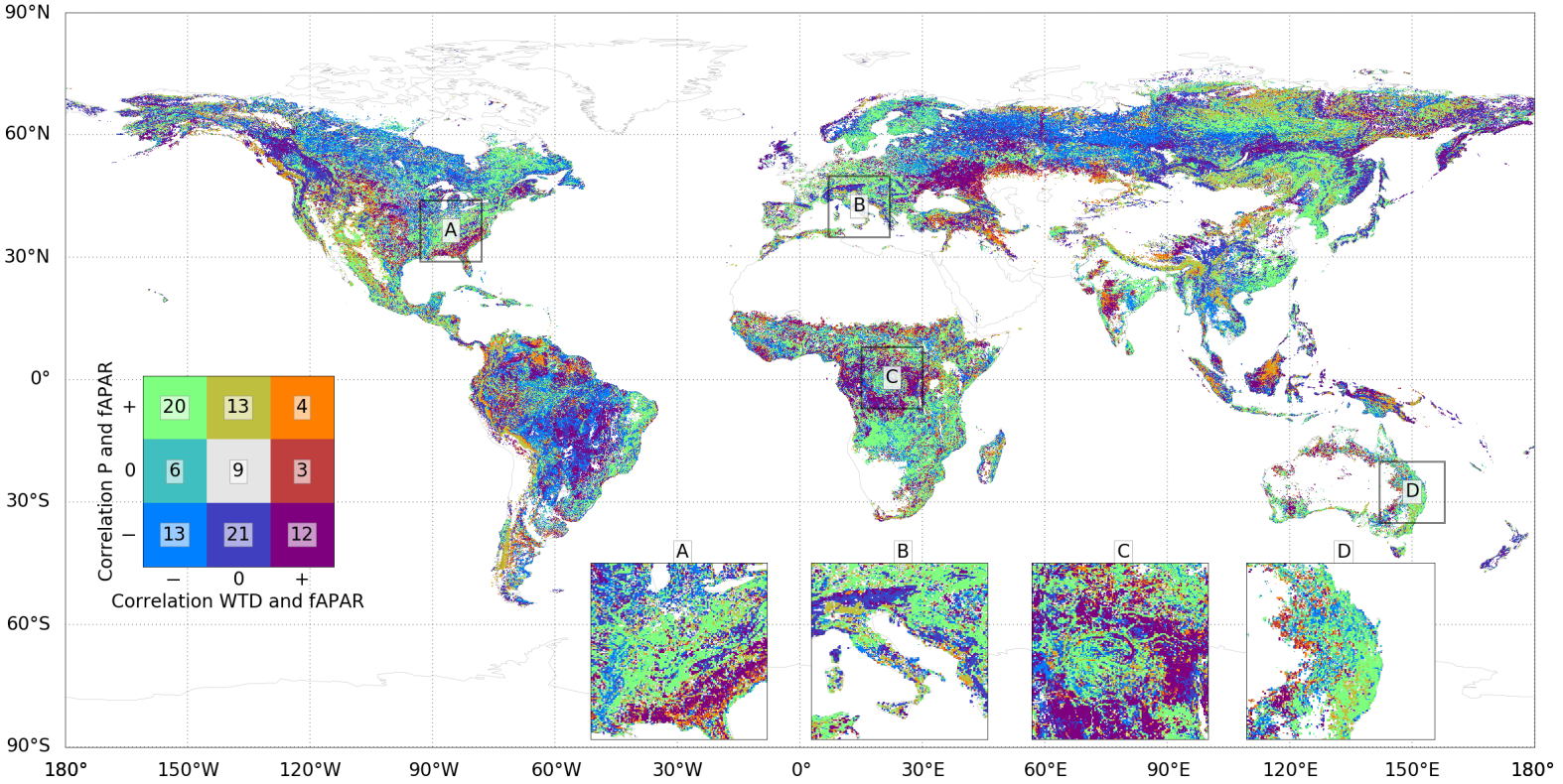

Figure S11. Global distribution of the ecohydrological classes. This is a bigger representation of the same figure displayed in the main paper. For an in depth explanation of the map and a definition of the colours see the first section of the results and Figure 2.

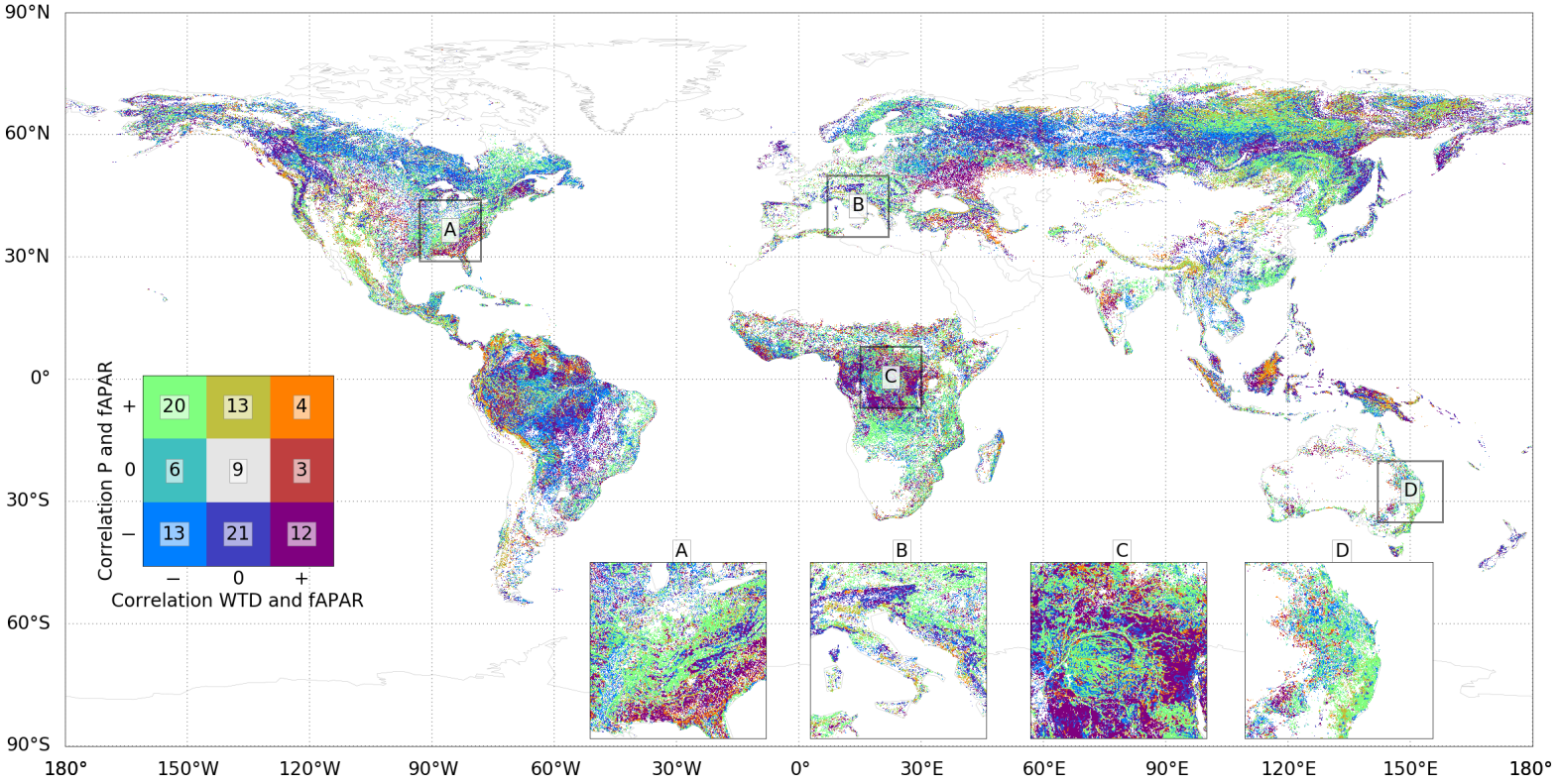

Figure S12. Global distribution of the ecohydrological classes at the full, 30 arc-second resolution.

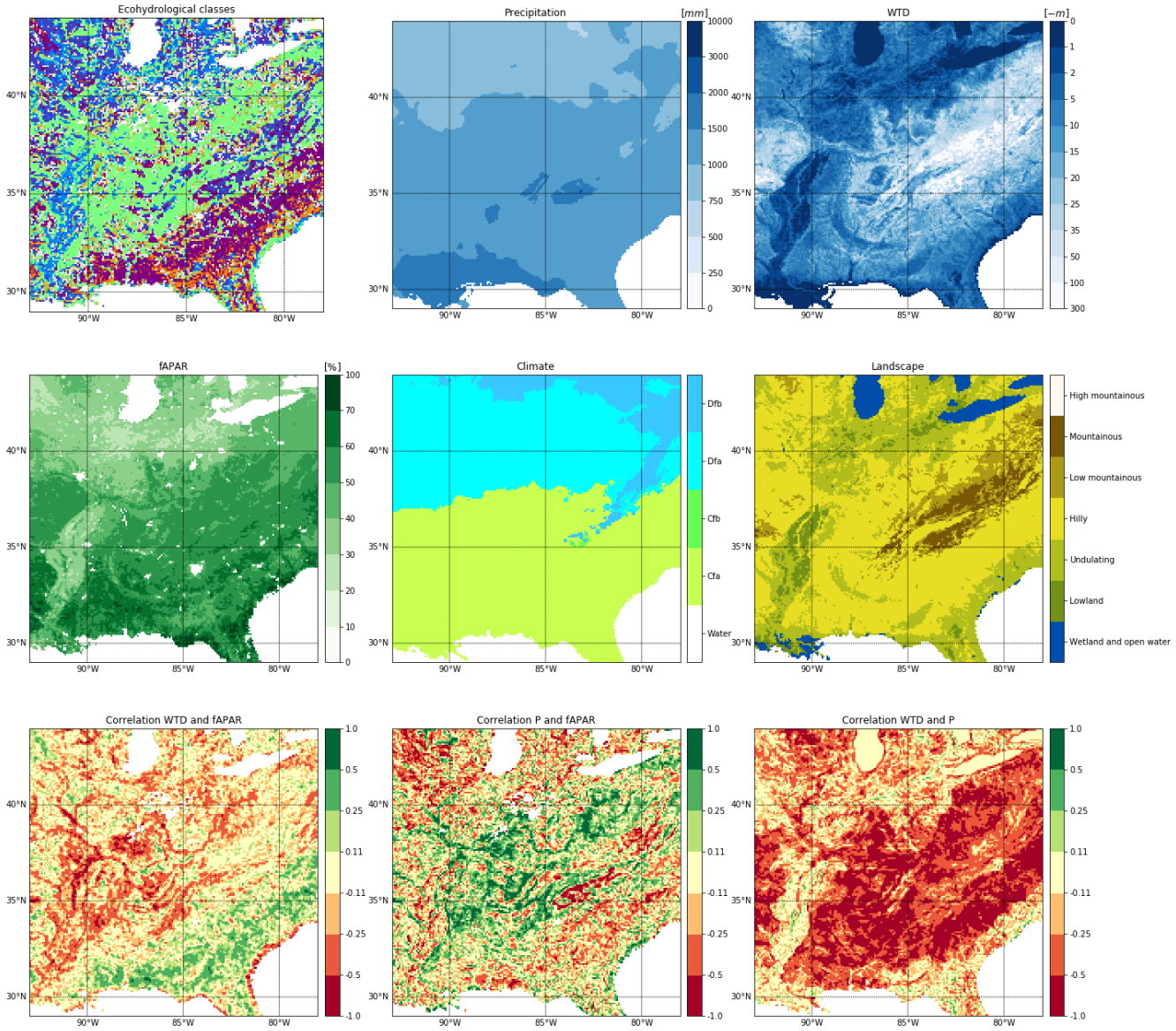

Figure S13. These maps depict the Mississippi river valley on the left and the southern part of the American East Coast on the right. For the interpretation of these figures see the main text.

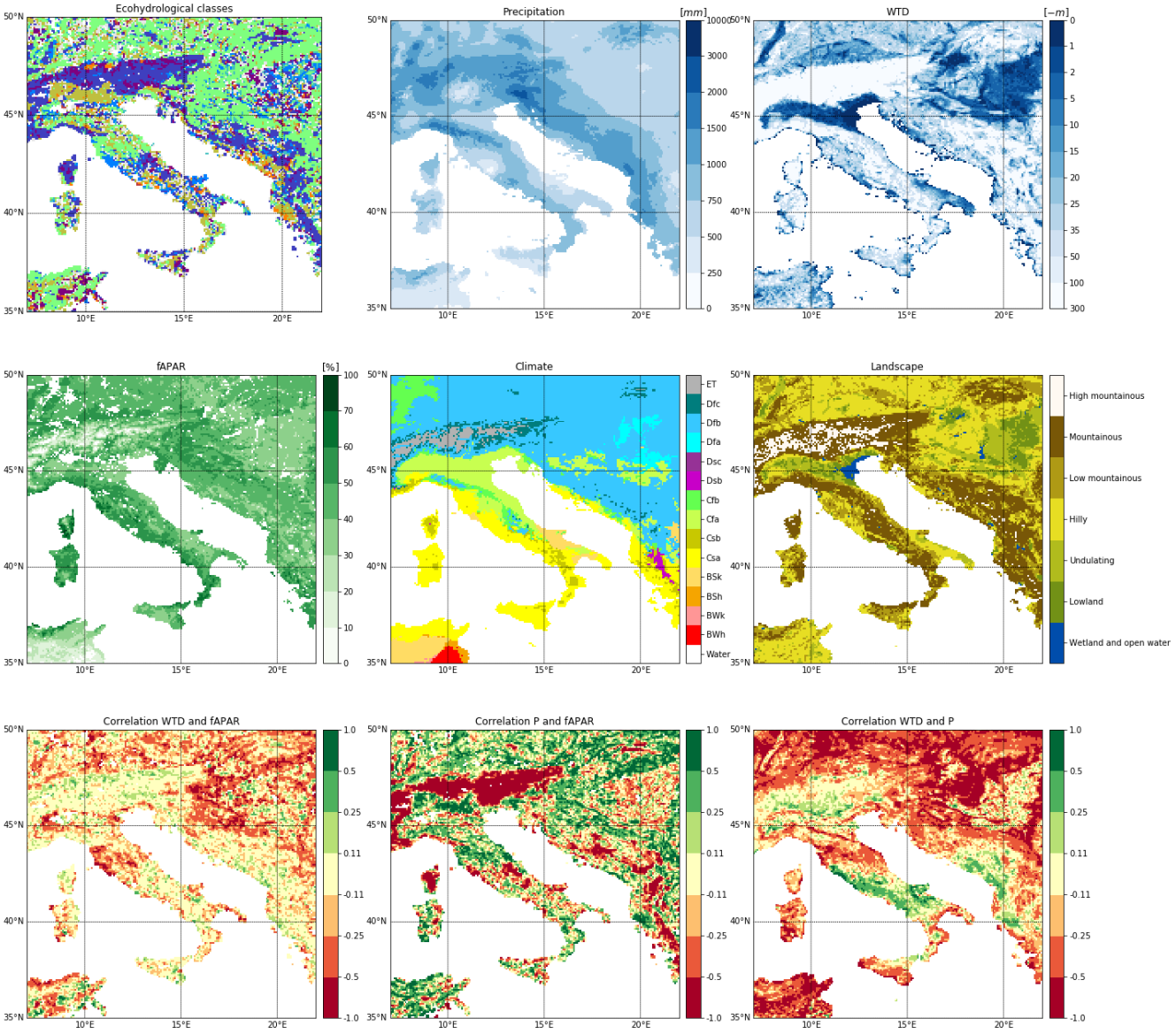

Figure S14. These maps depict South-Eastern Europe with the Alps. For the interpretation of these figures see the main text.

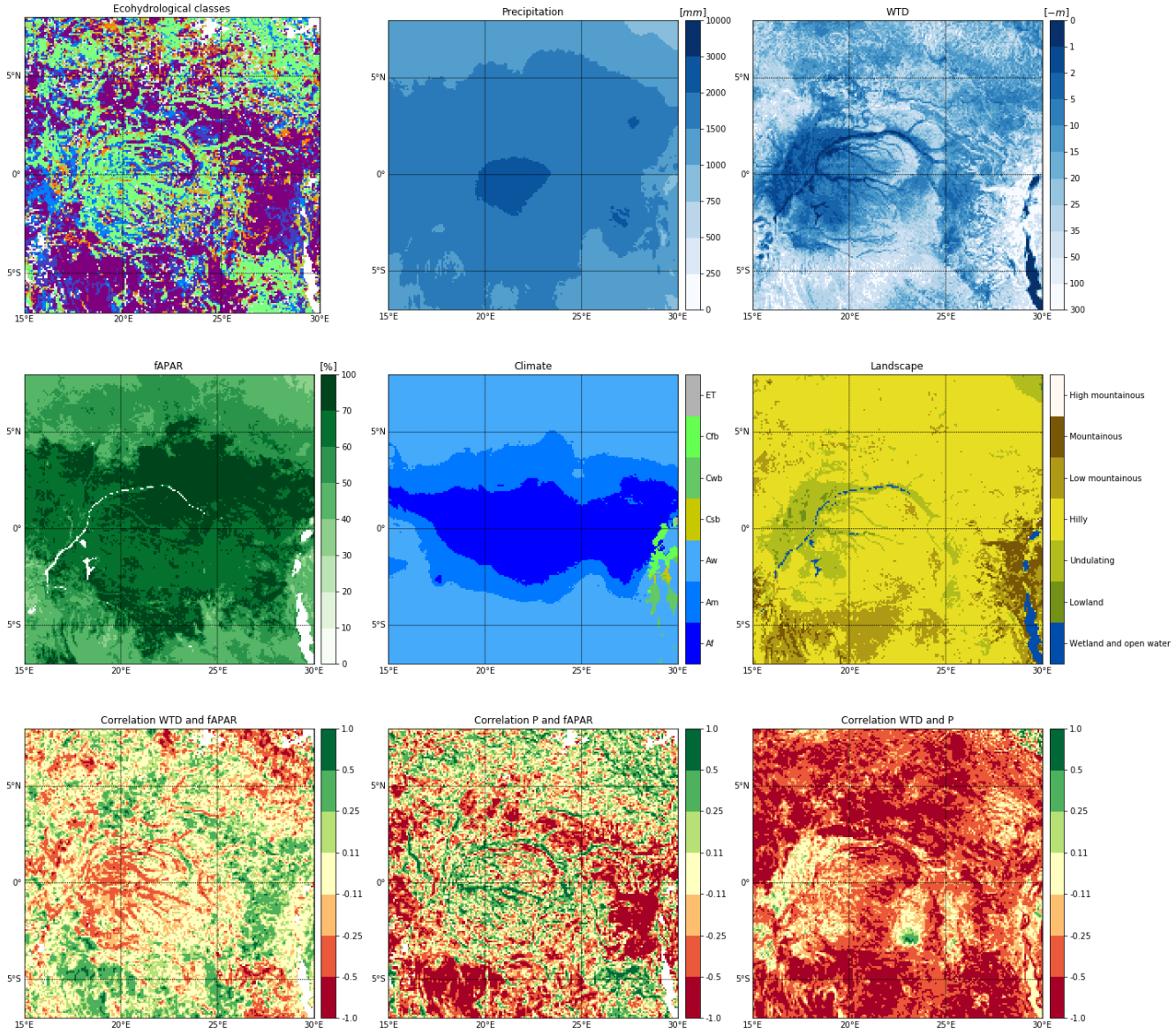

Figure S15. These maps depict the Congo river basin. For the interpretation of these figures see the main text.

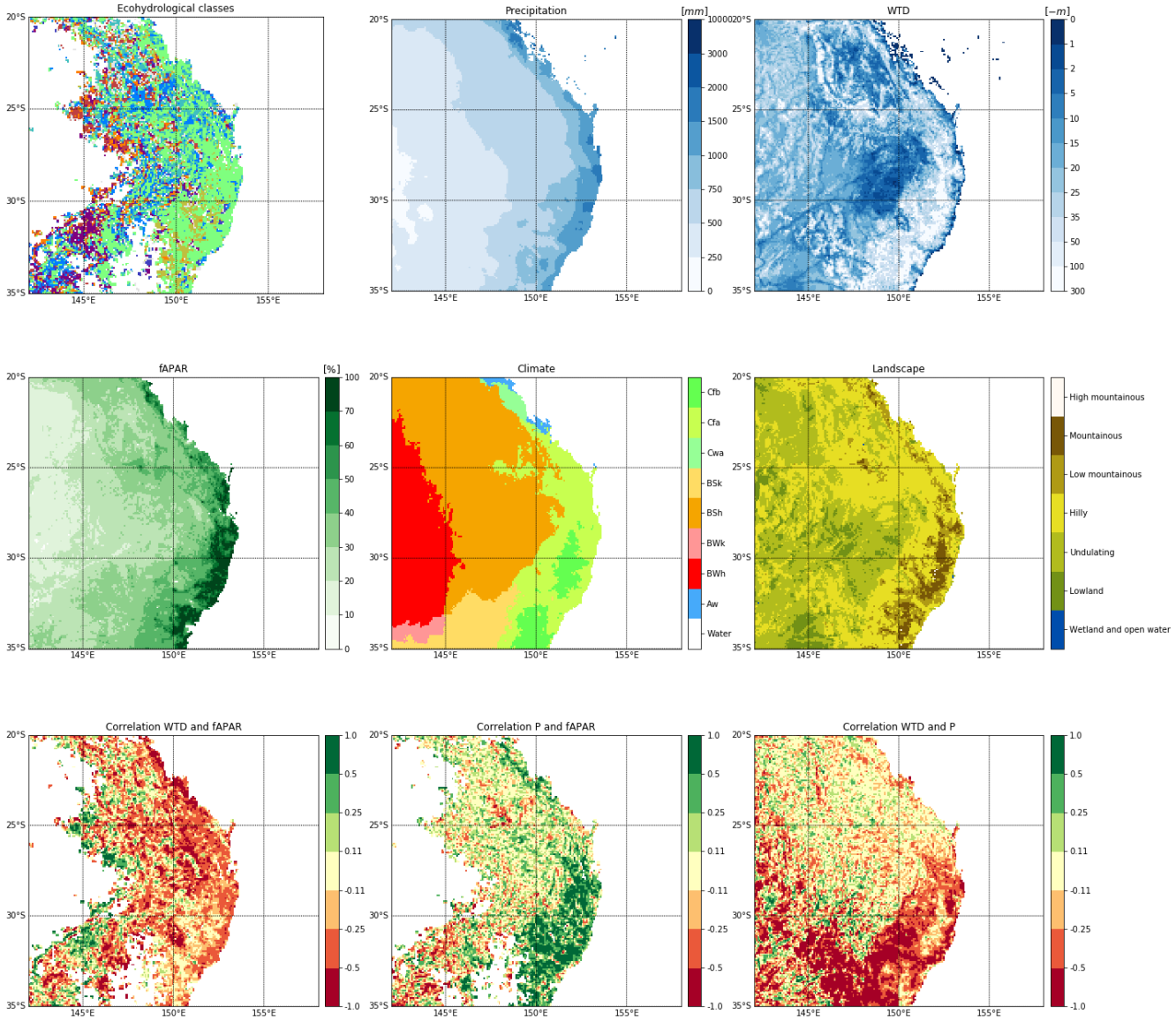

Figure S16. These maps depict Eastern Australia. For the interpretation of these figures see the main text.

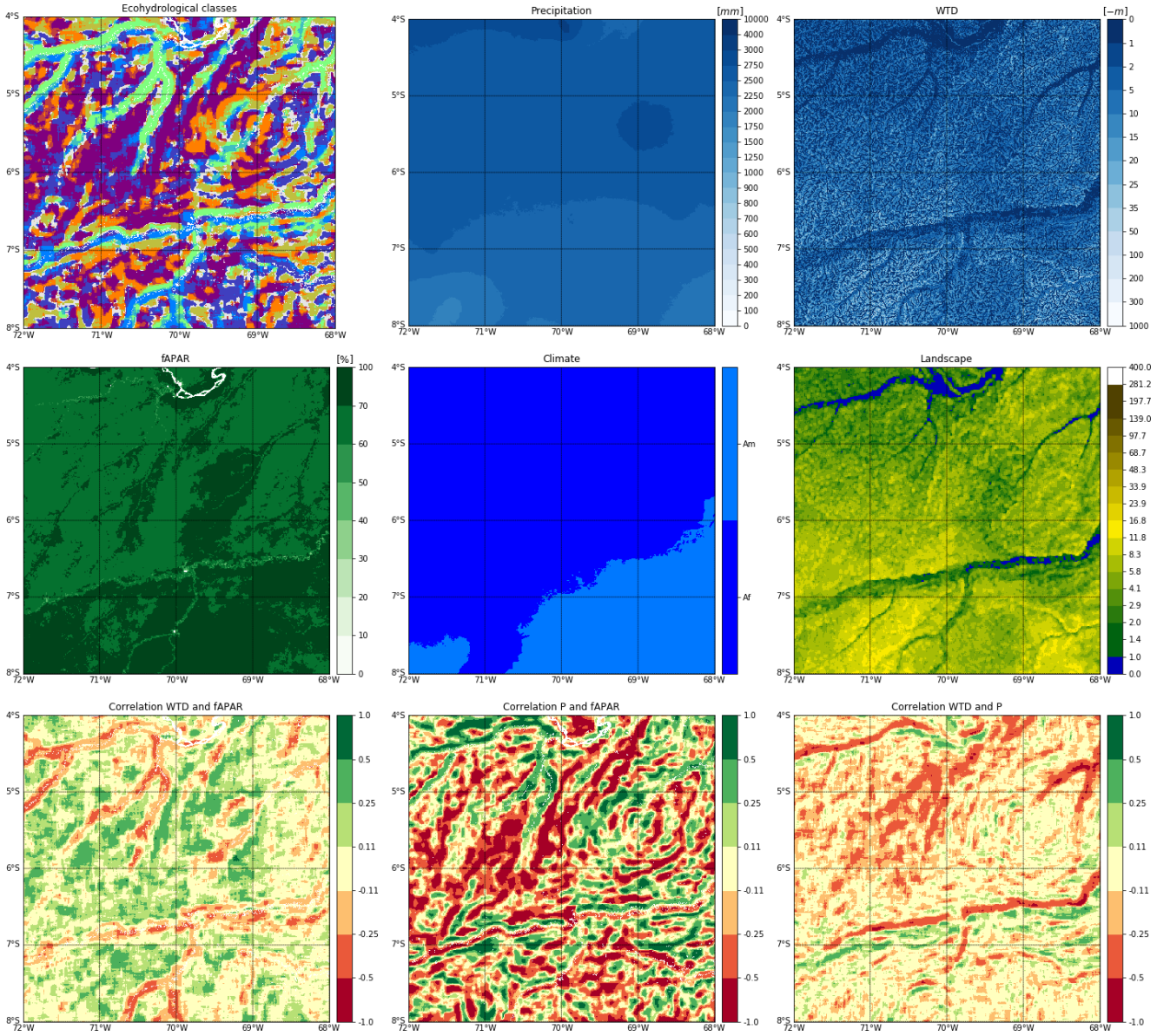

Figure S17. Subset of the data at their original resolution of 30 arc-seconds. The map depicts a part of the State of Amazonas in the west of Brazil. It displays a part of Figure 4 of the main paper of section 3.2, where the patterns displayed here are discussed.

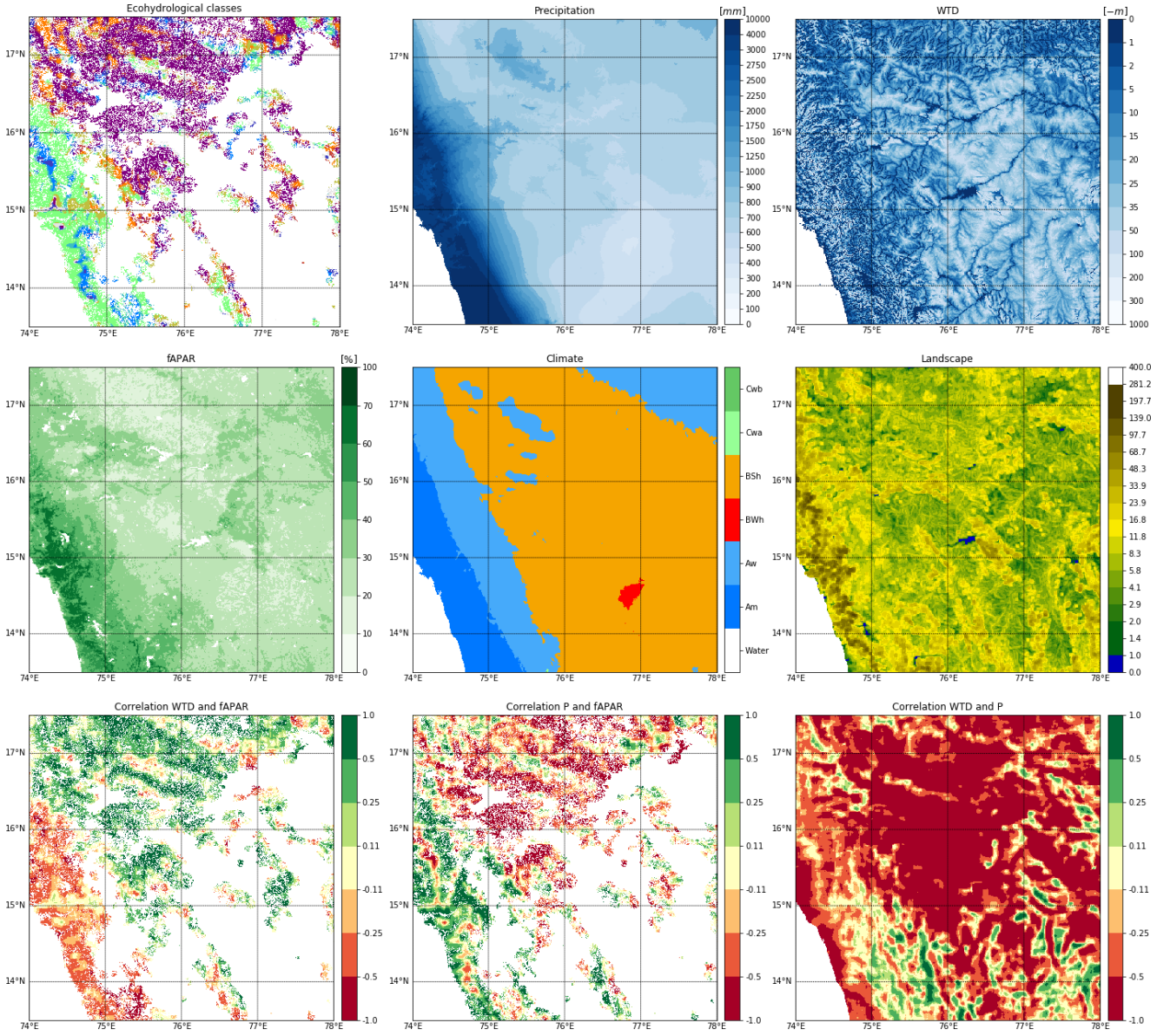

Figure S18. Subset of the data at their original resolution of 30 arc-seconds. The map depict a part of India, a subset of the maps displayed in Figure 5 of the main paper. In section 3.2 the patterns displayed here are discussed.

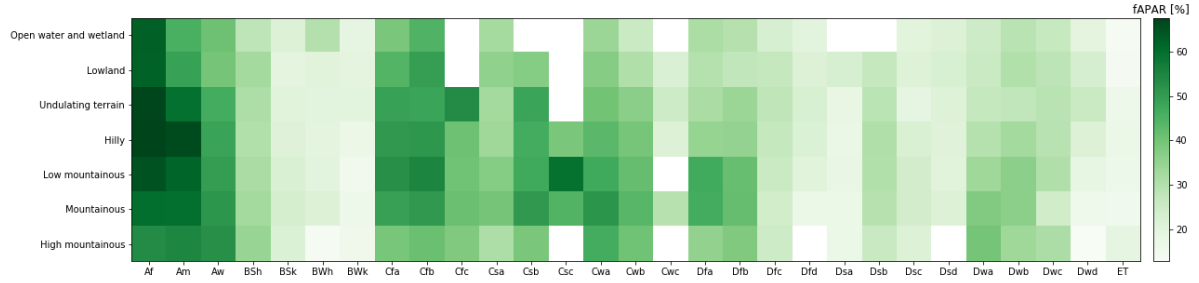

Figure S19. Mean fAPAR in different climate and landscape positions. White signifies that the combination of landscape and climate did not appear in the data.

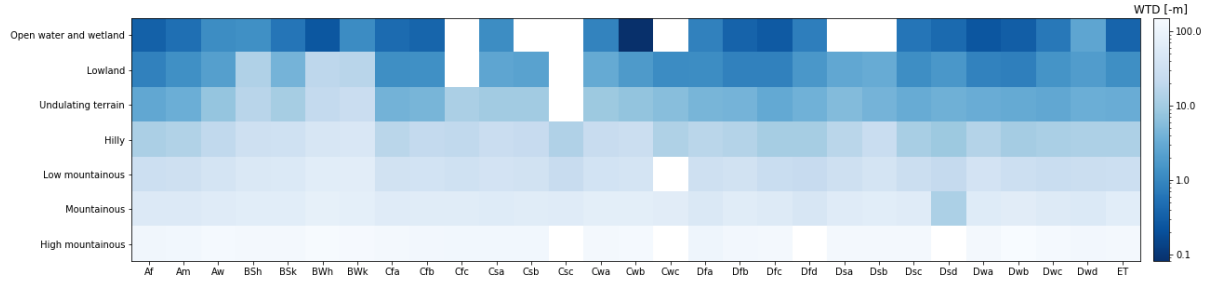

Figure S20. Mean fAPAR in different climate and landscape positions. White signifies that the combination of landscape and climate did not appear in the data.

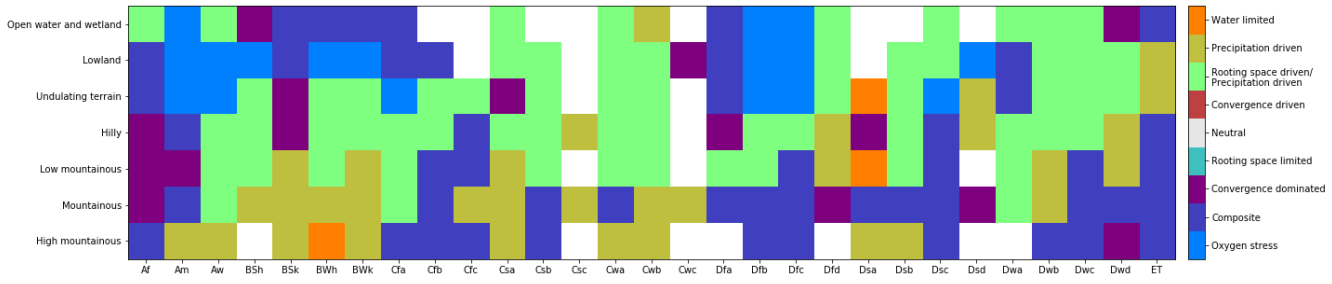

Figure S21. Prevalent class in different climate and landscape positions. For an explanation of the different classes see Figure 1 of the main text. White signifies that the combination of landscape and climate did not appear in the data or two classes are present in equal amounts.